Geophysical Journal International

Geophys. J. Int. (2016) **206,** 1221–1231
Advance Access publication 2016 May 29
GJI Seismology

doi: 10.1093/gji/ggw204

Inversion of surface wave data for subsurface shear wave velocity profiles characterized by a thick buried low-velocity layer

Daniela Farrugia,[1] Enrico Paolucci,[2] Sebastiano D'Amico[1] and Pauline Galea[1]

[1]*Department of Geosciences, Faculty of Science, University of Malta, Msida MSD*2080*, Malta. E-mail:* *daniela.farrugia@um.edu.mt*
[2]*Dipartimento di Scienze Fisiche, della Terra e dell'Ambiente, Università degli Studi di Siena, Siena, Italy*

Accepted 2016 May 26. Received 2016 May 23; in original form 2015 October 28

SUMMARY

The islands composing the Maltese archipelago (Central Mediterranean) are characterized by a four-layer sequence of limestones and clays. A common feature found in the western half of the archipelago is Upper Coralline Limestone (UCL) plateaus and hillcaps covering a soft Blue Clay (BC) layer which can be up to 75 m thick. The BC layer introduces a velocity inversion in the stratigraphy, implying that the V_{S30} (traveltime average sear wave velocity (V_S) in the upper 30 m) parameter is not always suitable for seismic microzonation purposes. Such a layer may produce amplification effects, however might not be included in the V_{S30} calculations. In this investigation, V_S profiles at seven sites characterized by such a lithological sequence are obtained by a joint inversion of the single-station Horizontal-to-Vertical Spectral Ratios (H/V or HVSR) and effective dispersion curves from array measurements analysed using the Extended Spatial Auto-Correlation technique. The lithological sequence gives rise to a ubiquitous H/V peak between 1 and 2 Hz. All the effective dispersion curves obtained exhibit a 'normal' dispersive trend at low frequencies, followed by an inverse dispersive trend at higher frequencies. This shape is tentatively explained in terms of the presence of higher mode Rayleigh waves, which are commonly present in such scenarios. Comparisons made with the results obtained at the only site in Malta where the BC is missing below the UCL suggest that the characteristics observed at the other seven sites are due to the presence of the soft layer. The final profiles reveal a variation in the V_S of the clay layer with respect to the depth of burial and some regional variations in the UCL layer. This study presents a step towards a holistic seismic risk assessment that includes the implications on the site effects induced by the buried clay layer. Such assessments have not yet been done for Malta.

Key words: Site effects; Crustal structure.

1 INTRODUCTION

The investigation of local ground conditions is an important part of seismic hazard assessment (Fäh *et al*. 2003). It is known that soft stratigraphic layers can greatly amplify ground motion in the event of an earthquake. Knowledge of the shear wave velocity (V_S) structure and/or the resonance frequency of the soft soil layers is an important step towards the prediction of ground motion, and hence in the prevention or mitigation of earthquake disasters (Arai & Tokimatsu 2004). Such information should contribute to earthquake-risk mitigation strategies such as seismic risk assessments, emergency response-preparedness and land use planning by considering existing and proposed buildings (Zor *et al*. 2010).

Direct measurement techniques, such as borehole logging and penetrometry, provide accurate information about subsurface geotechnical properties. Such invasive techniques, however, suffer from limitations that include the use of relatively expensive equipment and the difficulty in conducting measurements in urbanized areas because of the drilling involved. Due to their expensive nature, these techniques are usually limited in exploration depth. The traveltime average shear wave velocity in the uppermost 30 m (V_{S30}) is thus used for microzonation purposes and is adopted by several seismic design and building codes (e.g. Eurocode 8, EC8; Bisch *et al*. 2012) to evaluate potential site amplifications (Picozzi *et al*. 2009; Zor *et al*. 2010), even though statistical tests have shown that this parameter is not always a good proxy for seismic amplification (Castellaro *et al*. 2008; Gallipoli & Mucciarelli 2009), and deeper soil properties may have to be considered.

During the past few decades, passive seismic techniques which make use of the acquisition of ambient vibrations (or microtremors), assumed to be dominated by surface waves, have been developed and are becoming increasingly popular. These techniques are convenient because they provide quick reliable estimates of subsurface soils with good lateral coverage, utilizing relatively cheap equipment that can be easily deployed in urban areas (Parolai *et al*. 2005).

This study focuses on a particular type of stratigraphy which is prevalent and consistent over the western half of the Maltese archipelago. In this region, a layer of clays and marls, known locally as Blue Clay (BC), may exceed 70 m in thickness and underlies the topmost, youngest layer of the sedimentary sequence, a hard reef limestone varying in thickness from a thin covering of a few metres to more than 80 m. Where the uppermost layer has been eroded away, or along hill slopes, the clay may outcrop as a soft surface layer, which is expected to produce site amplification in a standard manner. This study is motivated principally by the need to understand how the built environment would respond to strong or moderate earthquake ground shaking in areas underlain by this buried clay layer, given that such areas are being increasingly built upon. An important input to the numerical prediction of such behaviour is an accurate analysis of the shear wave velocity profiles down to the base of the clay layer, and of the extent of its lateral variations. The clay is presumed to create a conspicuous shear wave velocity inversion in the profile.

The presence of a shallow thick low-velocity layer is not uncommon, especially in sedimentary environments encompassing clay deposits. However, studies of the effects of such stratigraphies on multimode inversion procedures as well as site effects and interpretation of site classes and parameters like V_{S30} are limited. Asten (2006) uses the MMSPAC (Multiple-Mode Spatial Auto-Correlation) technique, which involves fitting directly the observed SPAC curves to identify low-velocity layers in the near surface obtained in the Santa Clara Valley, California. Arai & Tokimatsu (2005) used the high-resolution f-k technique (Capon 1969) jointly with the H/V technique to obtain shear wave velocity profiles for sites in Japan. Di Giacomo *et al*. (2005) compared the H/V results obtained using earthquake data to noise H/V at Venosa (Italy) which again is characterized by a low-velocity layer. The implications of low-velocity layers on site class definition and hence on the correct prediction of their response to ground shaking are important in earthquake ground motion modelling and engineering issues. Yet the literature focusing on this issue and the effect of low-velocity layers on ambient noise measurements is minimal.

A previous study on the islands has yielded shear wave velocity profiles at a limited number of sites using the active Multichannel Analysis of Surface Waves (MASW) technique (Panzera *et al*. 2013). The depth resolution of this study was, however, limited to around 30 m, and the low-velocity clay layer was not adequately sampled in most of the cases. Other models of seismic-wave velocity profiles were made by inverting single-station H/V data in one area along the NE coast of the islands characterized by the same shear wave velocity inversion (Pace *et al*. 2011; Panzera *et al*. 2012).

This study attempts to improve on previous measurements by extending the number of measurement sites as well as by using more robust methods of data inversion. For this purpose, the passive multistation (array) Extended Spatial Auto-Correlation (ESAC; Ohori *et al*. 2002) technique has been used jointly with the single-station Horizontal-to-Vertical Spectral Ratio method (H/V or HVSR; Nakamura 1989, 2000) to infer 1-D V_S profiles at seven sites with the stratigraphy explained above, that is, with the presence of a thick, buried low-velocity layer on the two principal islands. The capacity of such inversion methods to adequately resolve such structures is also tested.

Better constrained shear wave velocity profiles will enable us to better understand the influence of this kind of geology on site amplification as well as the implications of the velocity inversion on the suitability of V_{S30} as a proxy for site response and the definition of site classes for engineering purposes. The V_S profiles obtained in this study will eventually be used to derive site-specific amplification functions for the computation of ground motion parameters for ad-hoc earthquake scenarios.

2 GEOLOGICAL SETTING

Located in the Central Mediterranean, the Maltese archipelago comprises three main islands—Malta, Gozo and Comino—formed as marine sediments during the Oligocene and Miocene epochs. The geology consists of four main strata of lime-rich sedimentary rocks, the lime content being present mainly due to the fossil shells of animals and plants which are found in abundance in the strata (Pedley *et al*. 2002 and references therein). Although the layers essentially lie horizontally, they are displaced by a dense network of faults across the islands, which also control the erosion of the exposed rock layers. Starting from the oldest, these are the Lower Coralline Limestone (LCL), the Globigerina Limestone (GL), the BC and the Upper Coralline Limestone (UCL; Fig. 1a). Even though the stratigraphic sequence in the Maltese islands is relatively simple, the properties of the layers vary locally.

The hard and compact pale grey LCL shapes the steep sided cliffs in the southwestern part of the islands. It is not homogeneous and presents a number of different facies. The GL is a soft yellowish fine-grained limestone, which is further subdivided into three layers separated by two thin hardground conglomerate layers. Although the BC is considered as a continuation of the GL, this layer has a higher clay mineral content which prevents the binding of the particles, thus making this layer the softest in the layer package and easily erodible. In a few areas around the islands, one also finds a thin layer of bioclastic limestones named the Greensand Formation, which varies from 1 to 11 m in depth. The youngest of the layers, that is, the UCL, is a reef limestone, which, as indicated by the name, has properties very similar to the LCL. The UCL is also highly variable, ranging from fractured and friable to highly compact.

As can be seen from the geological map of the islands (Fig. 1b), in the eastern half of Malta the two youngest layers (BC, UCL) are missing and the area is characterized mostly by outcropping GL, giving rise to a flat, rolling landscape in this part of the islands. On the other hand, the western half of Malta and some areas in Gozo retain the full sedimentary sequence (Pedley *et al*. 2002), with UCL hillcaps and plateaus overtopping BC gentle slopes being a dominant feature in the landscape of northwestern Malta and northeastern Gozo (Gigli *et al*. 2012).

The Maltese archipelago is affected by low-to-moderate seismic hazard. Since 1530, at least four earthquakes of intensity VII or VII–VIII on the European Macroseismic Scale (EMS-98) were experienced, with the major contributor to the seismic hazard being the northern segment of the Malta Escarpment (Galea 2007). Felt and damaging earthquakes can also be attributed to active fault zones in the Sicily Channel and the Hellenic Arc (e.g. Agius *et al*. 2015). The last damaging earthquake occurred over a century ago, when the islands were still sparsely built up compared to today's building density. During the last couple of decades building heights of more than five storeys, usually incorporating large open basements acting as garages, have become increasingly common. The majority of the building stock is of load-bearing unreinforced masonry, which is vulnerable even to moderate ground shaking. Furthermore, the building footprint has also spilled to geologically unstable areas characterized by the presence of clay. The public perception is one

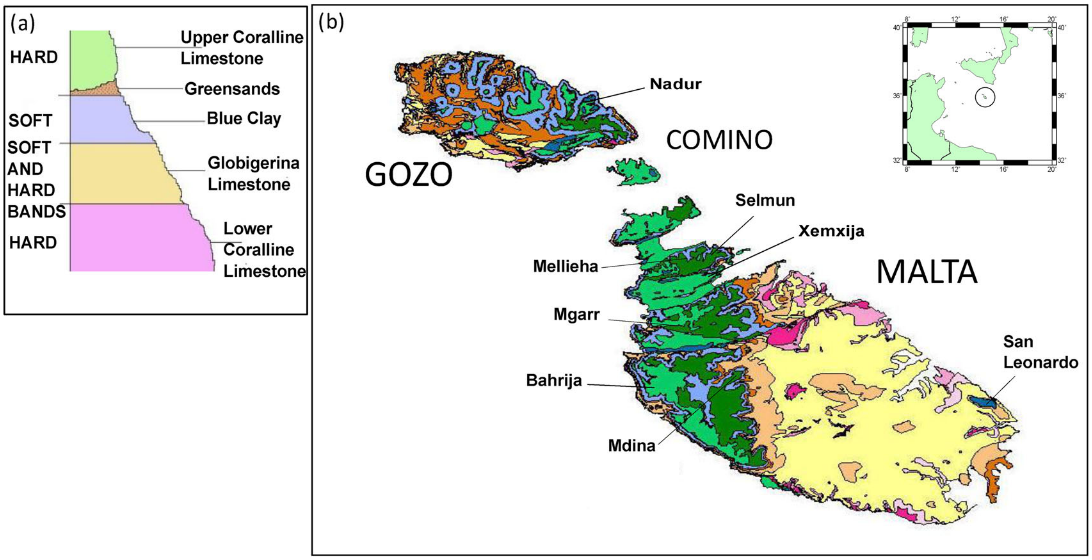

Figure 1. (a) A sketch of the full sedimentary sequence making up the islands above sea level. (b) The geology map of the Maltese islands together with the location of the chosen sites for investigation. The different shades of green correspond to the different members of the UCL. Inset shows the position of the Maltese islands (in circle) in the Mediterranean Sea.

of unjustified complacency, and no comprehensive assessment of seismic risk has so far been carried out (Galea 2007). In addition, the islands remain by far the most densely populated member state of the European Union with an average of around 1300 persons per km^2. For a small island state, such as in this case, the social and economic impacts of a damaging earthquake are considerable.

3 DATA ACQUISITION AND ANALYSIS

3.1 The investigated sites

The main aim of this study is to use passive seismic surface wave methods to derive shear wave velocity profiles at sites where the BC is overlain by the UCL, a very common scenario in the northern and western part of the islands. Seven sites have been chosen for this investigation (six in Malta and one in Gozo, shown in Fig. 1b), all of which are characterized by the full sedimentary sequence, that is, the BC is embedded between the UCL above and the GL from below (refer to Fig. 1). By choosing sites of similar stratigraphy in different parts of the islands, we could also investigate any spatial geophysical variations within a particular stratum. The sites for array measurements were chosen to have no major topographical slopes or irregularities.

One of the chosen sites, Mdina, is the former capital city of Malta—a heavily urbanized fortified town built on a hill with a thin outcropping UCL layer (with a maximum thickness of around 6 m) protecting the erodible BC. A very thin layer (less than 1 m) of Greensand is also present (Gigli *et al*. 2012). The city has previously suffered serious damage from major earthquake events, in particular, the Sicily Channel M 7.4 earthquake of 1693 January 11. This event produced an intensity of VII–VIII, and various buildings suffered serious damage (Galea 2007; Gigli *et al*. 2012). Other sites were in a more rural environment, but always close to inhabited areas. At each site, a number of single-station ambient noise measurements were conducted jointly with the array measurements.

In addition, measurements were also conducted on a small area in the SE of Malta, called San Leonardo, which is the only known site on the islands where the UCL directly overlies the GL, that is, the BC is not present in the geological sequence (Zammit-Maempel 1977; Pedley 2011). This area offers the best opportunity to validate the results obtained in the presence of the buried BC.

3.2 Single-station H/V measurements

A number of three-component single-station recordings of ambient seismic noise were conducted close to the deployed arrays (refer to Fig. 2 and the next section) using the digital tromograph Micromed Tromino™ (www.tromino.eu). The Tromino is a compact, battery-operated, all-in-one system composed of three orthogonal velocity sensors and 24-bit digitizer, whose sampling frequency extends up to 1024 Hz. The manufacturer's specifications indicate that the Tromino may be used at frequencies down to 0.1 Hz (sensor frequency range 0.1–300 Hz). Time-series of 20 min each, sampled at 128 Hz, were analysed using the software Grilla™ to obtain H/V curves in the frequency range of 0.5–64 Hz as described in Vella *et al*. (2013). The time-series were divided into 60 non-overlapping windows, each 20 s long, as suggested by the SESAME guidelines (Bard 2005). Any window containing spurious signals was removed before the analysis so that the standard deviation was minimized. The H/V curve was obtained by averaging the horizontal spectra using the geometric mean and dividing by the vertical spectrum for each time window. The curves for each window were then averaged to get the final H/V curve. The whole procedure is described more thoroughly in Picozzi *et al*. (2005).

The frequency at which the H/V curve shows a valid peak corresponds to the fundamental frequency of the site (Bonnefoy-Claudet *et al*. 2006). Although the theoretical basis of the origin of this peak is still debatable, the method is widely used for site investigations due to its capability of estimating the fundamental resonance frequency of a site, f_0, which is related to the ratio of the traveltime average shear wave velocity $\langle V_S \rangle$ of a surface sedimentary cover with thickness H above the bedrock by

$$f_0 = \frac{\langle V_S \rangle}{4H}. \quad (1)$$

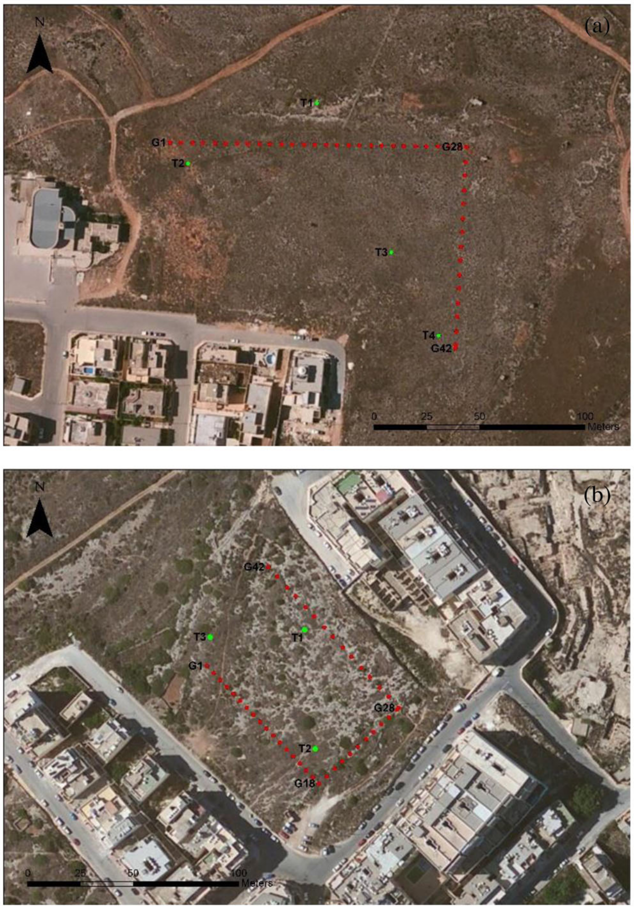

Figure 2. The array setup at (a) Bahrija and (b) Xemxija. The red dots show the position of each geophone while the Gxx at the corners of each array indicate the number of the geophone found in that corner. The Tx refer to the sites where the single-station H/V recordings were obtained. (Images produced on Google Earth.)

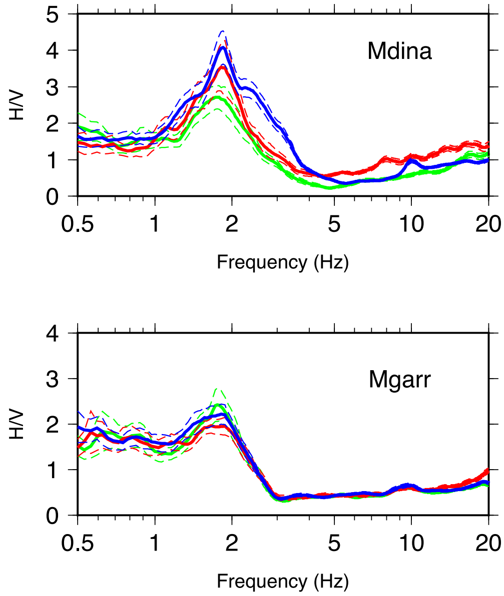

Figure 3. All the H/V curves obtained at Mdina and Mgarr with confidence intervals (dashed lines).

The fundamental frequency is generally well detected and consistent with that predicted using 1-D *SH*-transfer function computation, however, various studies have shown that the H/V tends to underestimate the amplification values (Satoh *et al*. 2001; Bonnefoy-Claudet *et al*. 2006).

In order to determine whether the sampled area beneath the array consists of approximately homogeneous strata, various single-station readings were taken close to the array itself. If all H/V curves peaked at the same frequency and had similar shapes, this was taken as an indication that the sediment cover was uniform over the extent of the array, satisfying one of the key assumptions of the array methods. An example of this is given in Fig. 3.

3.3 Multistation measurements

The passive seismic array measurements were conducted using Micromed SoilSpy Rosina™ seismic digital acquisition system equipped with 4.5 Hz vertical geophones. A total of 42 geophones were used, and placed in an L- or C-shaped configuration with a regular interstation distance of 5 m. At the Mdina and San Leonardo sites, only 17 geophones were employed because of space limitations. Fig. 2 shows the deployment at Bahrija and Xemxija. Even though such instrumentation (use of strings of 4.5 Hz geophones) and configuration is not ideal, it has been shown in various studies that reasonable results, and consistent with borehole data (whenever available), can be obtained (e.g. Albarello *et al*. 2011; Hayashi *et al*. 2016).

Since only vertical sensors were used, the signals detected are interpreted as plane Rayleigh waves in their fundamental and higher propagation modes. The recordings, each 20 min long and sampled at 256 Hz, were analysed using the ESAC technique and the curves automatically picked by the provided code (Ohori *et al*. 2002; Okada 2003; Parolai *et al*. 2006; Albarello *et al*. 2011).

The ESAC technique provides a unique 'effective' dispersion curve (Rayleigh-wave phase velocity versus frequency). If the wavefield consists of fundamental mode Rayleigh waves, then the curve represents the Rayleigh-wave dispersion curve. However, in the presence of higher mode Rayleigh waves, the curve would contain contributions from higher modes of propagation that cannot be resolved due to limited resolution of the finite array (Foti *et al*. 2015). The use of an effective dispersion curve avoids the picking of the different propagation modes which can be problematic (Albarello *et al*. 2011; Ikeda *et al*. 2012).

3.4 Data inversion

The 1-D V_S profiles were obtained by inverting both H/V and effective dispersion curves in a joint inversion procedure based on the Genetic Algorithm (GA; Yamanaka & Ishida 1996; Picozzi & Albarello 2007). Proposed by Parolai *et al*. (2005) and Arai & Tokimatsu (2005), the joint inversion procedure utilizes the two data sets, which are sensitive to different properties and thus information about the deeper part of the profile, which is not captured in the low-frequency part of the dispersion curve, can be obtained (e.g. Asten *et al*. 2014). Scherbaum *et al*. (2003) show that while the dispersion curve constrains the V_S of the sedimentary cover, the thickness, *H*, is better constrained by the H/V peak frequency. Various studies (e.g. Shabani *et al*. 2008; Picozzi *et al*. 2009; Albarello *et al*. 2011; Panzera & Lombardo 2012; Panzera *et al*. 2013) have used the joint inversion technique since its proposal. It has been shown to give reliable results, usually closer to the available geotechnical data than the ones obtained using conventional inversion procedures.

Table 1. The inversion limits used for the Mellieha data concerning thickness and V_S values. In this case, the first two layers correspond to the UCL, the third, fourth and fifth represent the Blue Clay, Globigerina Limestone and Lower Coralline Limestone respectively. Layers 6–8 (in the grey-shaded box) are added so as to avoid biases in the forward computation.

Layer number	Thickness limits (m)	V_S limits (m s^{-1})
1	5–15	400–1500
2	10–60	400–1500
3	10–60	400–1500
4	20–80	700–1800
5	50–100	800–2000
6	200–300	1000–2500
7	100–1000	1000–2500
8	0	1000–3000

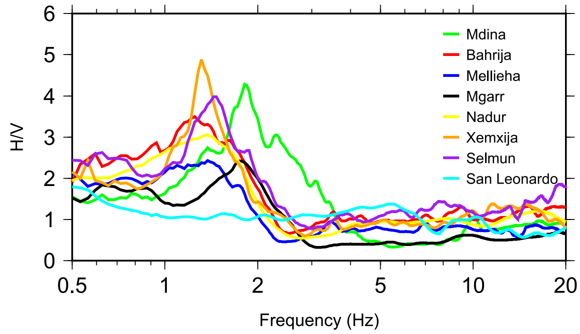

Figure 4. The representative H/V curves obtained at the seven sites characterized by a low-velocity layer and one obtained at San Leonardo site.

Sensitivity analyses (Tokimatsu 1997; Xia *et al.* 1999) have shown that the Rayleigh-wave dispersion and H/V curves are mostly influenced by V_S and H, rather than by the density ρ and P-wave velocity, V_P. As a consequence, in order to reduce the variability of the inversion results, it has been decided to link the value of ρ to that of V_P as in Boore (2015). The V_P was allowed to vary between 200 m s^{-1} and 3000 m s^{-1}, while the density varied between 1500 kg m^{-3} and 2500 kg m^{-3} in all cases.

The range of values of the most important parameters in the inversion, namely layer thickness and shear wave velocity, for each site inversion were guided by previous knowledge of the site geology, from geological maps or previous publications. In each inversion, the number of layers, of variable thickness, was kept fixed (with a minimum of four layers above the half-space), however an additional couple of layers were added at the bottom of the model to avoid unrealistic mode truncation in forward computation, since this computation takes into account surface waves only (Picozzi & Albarello 2007). The shear wave velocity in each layer was allowed to vary over a wide range of values, with no *a priori* assumption about the presence or nature of a low-velocity layer. This enabled us to assess the ability of the GA to correctly identify and characterize the shear wave velocity inversion. Table 1 shows one example of the limits used in the Mellieha case.

Theoretical HVSR and effective dispersion curves have been computed on the basis of the model proposed by Lunedei & Albarello (2009). In particular, the authors assume the subsoil to be a flat stratified viscoelastic medium where only surface waves (Rayleigh and Love) propagate. From this model, both theoretical HVSR and effective dispersion curves can be computed from the above-mentioned set of parameters representative of the subsoil (thickness, V_S, V_P, and density).

In each inversion process, higher propagation modes were considered. It is known that at sites where the V_S varies irregularly with depth (e.g. in the presence of a stiff layer overlying a soft layer), higher modes can dominate certain frequency ranges (e.g. Tokimatsu 1997; Zhang & Lu 2003; Arai & Tokimatsu 2004). The inclusion of their effect in the inversion process stabilizes the process and increases the resolution of the inverted V_S profiles. Moreover, higher modes are more sensitive to the deeper structure than the fundamental one and thus increase the resolvable depth of the profile (Xia *et al*. 2003). Ikeda *et al*. (2012) proposed two inversion schemes which take into account the effect of higher modes by using the amplitude response of each mode, so that misidentification in mode picking is avoided. In the present work, higher modes up to $n = 10$ are taken into account via the effective dispersion curve. The effective dispersion curve for a given model is here computed following the procedure outlined in eq. (2) of Lunedei & Albarello (2009).

The GA is an iterative procedure which focuses exploration in the more promising areas within a research space (Albarello *et al.* 2011). From the initial 100 randomly generated models, a number of best models are selected and genetic operators (cross-over, mutation and elite selection) are applied to simulate genetic selection and create a second generation of models. The processes were repeated through 150 iterations, except in the case of Nadur where 300 generations were used to better enable the misfit to reach an acceptable minimum. For each site, ten separate inversions were run and the best-fitting profile for each was saved. The final result was chosen as the one characterized by the minimum misfit value (i.e. whose synthetic H/V and effective dispersion curves best fit the experimental ones, in accordance with the established measures) from all 10 inversions. The other best results are useful to estimate the inversion result variability and robustness.

4 RESULTS AND DISCUSSION

4.1 H/V curves

Fig. 4 shows the H/V curves obtained at the seven sites characterized by a velocity inversion together with one obtained at San Leonardo. The former sites exhibit a peak between 1 and 2 Hz, the amplitude of which varies between 2 and 5. Other studies carried out on the islands (Pace *et al*. 2011; Panzera *et al*. 2013; Vella *et al*. 2013; Galea *et al*. 2014) have also observed this ubiquitous peak wherever the soft BC is found underlying the compact UCL. This resonance is presumably associated with the boundary separating the BC and the GL (Panzera *et al*. 2012) and decreases in frequency with increasing depth of this boundary (Pace *et al*. 2011). Moving to high-frequency values, the peak is immediately followed by a drop below 1 in the H/V spectrum over a wide frequency range (Figs 3 and 4). This has been attributed to the presence of a velocity inversion in the stratigraphy (Di Giacomo *et al*. 2005; Castellaro & Mulargia 2009) and is also evident and consistent in all previous studies of areas of similar lithostratigraphy on the islands.

The curve obtained at San Leonardo site (where UCL outcrops but the BC layer is missing) contrasts with those where the BC is present as it is flat with no valid peaks above two units. Although the curve drops below 1, this is not observed for a wide range of frequencies (Fig. 4). We therefore conclude that the characteristics of the previous curves may indeed be attributed to the presence of the BC layer.

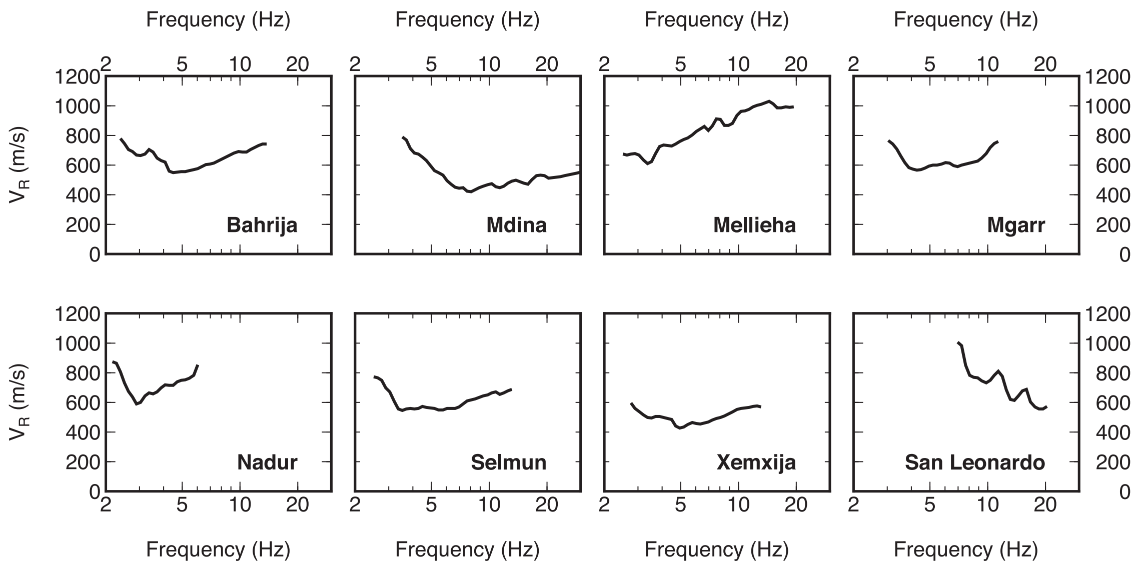

Figure 5. The effective dispersion curves (Rayleigh-wave phase velocity (V_R) versus frequency) obtained at the eight study sites.

4.2 Dispersion curves

Fig. 5 shows the resulting effective dispersion curves at each of the seven sites and San Leonardo. In the presence of higher modes, an effective (or apparent) dispersion curve will include a combination of the dispersion curves relative to the relevant modal components (Tokimatsu 1997). At lower frequencies, in the ranges that generally vary between 3–8 Hz and 3–5 Hz, the curves exhibit normal dispersion characteristics because the effective Rayleigh-wave phase velocity decreases with increasing frequency. At higher frequencies, this trend changes to an overall inversely dispersive one, that is, velocity increasing with frequency, which various authors attribute to the presence of a stiff layer overlying a softer one (i.e. UCL and BC, in this case; e.g. Tokimatsu 1997; Arai & Tokimatsu 2005). This shape of the effective curves is indicative of the presence of higher modes of surface waves. Although present in other situations, the presence of higher modes in this case may be associated with the presence of the buried low-velocity layer (Zhang & Lu 2003). In Mellieha, only an inversely dispersive curve was obtained suggesting that the combined UCL and BC layers are too thick for the GL to be adequately sampled with the given array configuration. Using an array with a larger aperture and geophones with a lower eigenfrequency, might improve the low-frequency part of the dispersion curve.

In contrast with these sites, the curve obtained at San Leonardo (bottom right in Fig. 5) shows a general decrease in phase velocity with frequency. At the highest attainable frequency, the obtained Rayleigh-wave velocity is around 600 m s^{-1}. At lower frequencies, the velocity continues to increase until it reaches 1000 m s^{-1} and never goes below 600 m s^{-1}, indicating that the topmost layer has the lowest velocity in the stratigraphy, and confirming the lack of the BC layer in this area.

4.3 The shear wave velocity profiles

The results of the joint inversion for all sites are summarized in Fig. 6, where the final profiles are displayed; the red profile indicating the best-fitting (i.e. lowest misfit) profile. The San Leonardo site is not included in this figure because the absence of the clay layer means there is no velocity inversion, which is the main object of this study.

A good match between the theoretical and experimental effective dispersion curves and H/V peak can be observed in all cases, except in Nadur (Gozo) where the theoretical resonance frequency is slightly lower than the experimental one. The UCL and BC thickness obtained in Mdina is in agreement with Gigli *et al*. (2012). Moreover, the resulting UCL thicknesses in the other sites are in consonance with the borehole data available (Government of Malta 1958).

A notable feature of the 10 final profiles in each inversion is that they are all in agreement on both the position of the low-velocity layer, and its velocity. Considering the fact that broad exploration ranges were initially associated with the layers in the parametrizations and that no *a priori* constraint of a low-velocity layer was made, such an agreement in all the models at the respective sites shows the robustness of the inversion and again indicates the sensitivity of the curves to the presence and properties of the low-velocity layer. In addition, this justifies the use of global search methods, such as the GA, which are able to retrieve reasonable profiles without the need of an initial profile close to the solution.

On the other hand, this consistency diminishes in the prediction of the velocity of the UCL and more so of the GL layer, where values between 700–1800 m s^{-1} were obtained. This inconsistency can be attributed to different facts: the available array conditions, especially length and resonance frequency of geophones which limit the observable depth; the soft BC layer acting as a high-pass filter and the trade-off that exists between the V_S and H in eq. 1 (Scherbaum *et al*. 2003).

The final profiles related to the best models reveal a variation in the UCL and BC shear wave velocities at the different sites. Table 2 lists the overall best model values and the ranges corresponding to the best-fit models from the 10 inversions. While the V_S in clay is around 400 m s^{-1} in Mdina, where the thickness of the UCL is less than 10 m, this value increases at the other sites and reaches a maximum value of 550 m s^{-1} in Mellieha, where the thickness of the overlying hard layer is around 56 m. This phenomenon can presumably be related to the overburden of the hard UCL layer on the BC, increasing the compactness of the particles, and thus the V_S of the layer. These velocities also contrast with those obtained

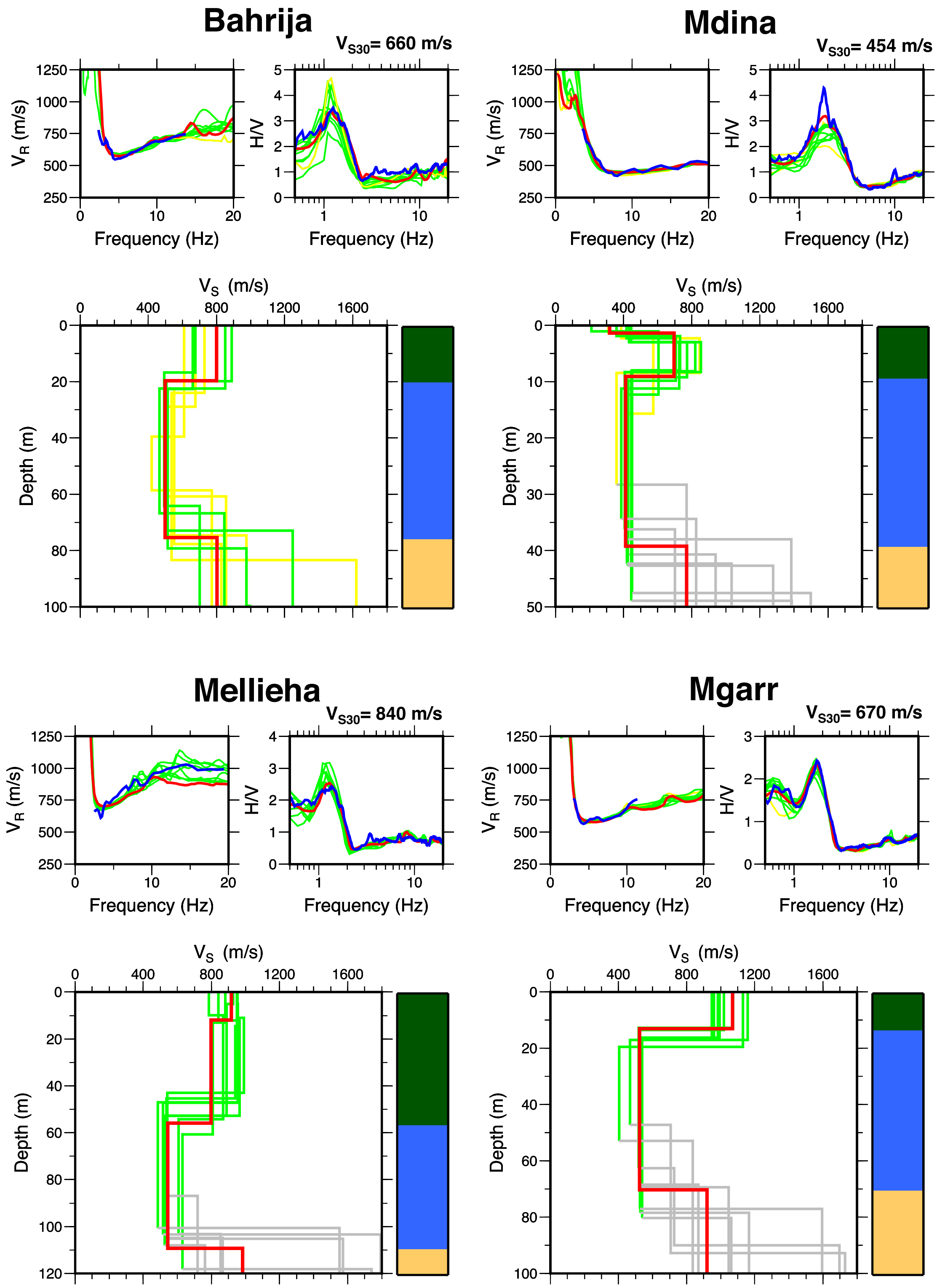

Figure 6. The joint inversion results and stratigraphic interpretation (lower panel) for Bahrija, Mdina, Mellieha and Mgarr sites. For each site, the best profiles from each of the 10 inversions are shown, with the red profile representing the one with the lowest misfit. The profiles in green are those characterized by a misfit which is within 50 per cent of the best model's misfit value; the yellow ones are characterized by a misfit greater than 150 per cent of the best model's misfit value. The GL layers are displayed in grey since the values are not reliably constrained by the data (refer to the text). Shown in the upper panel for each site are (from left to right) the effective dispersion and H/V curves. The blue curve is the experimental curve, the red curve shows the best-fitting theoretical curve while the rest (green and yellow) correspond to the other nine profiles. The calculated V_{S30} for each site is displayed in the top right corner. The colours used in the stratigraphic interpretation correspond to the colours in the geological map (Fig. 1).

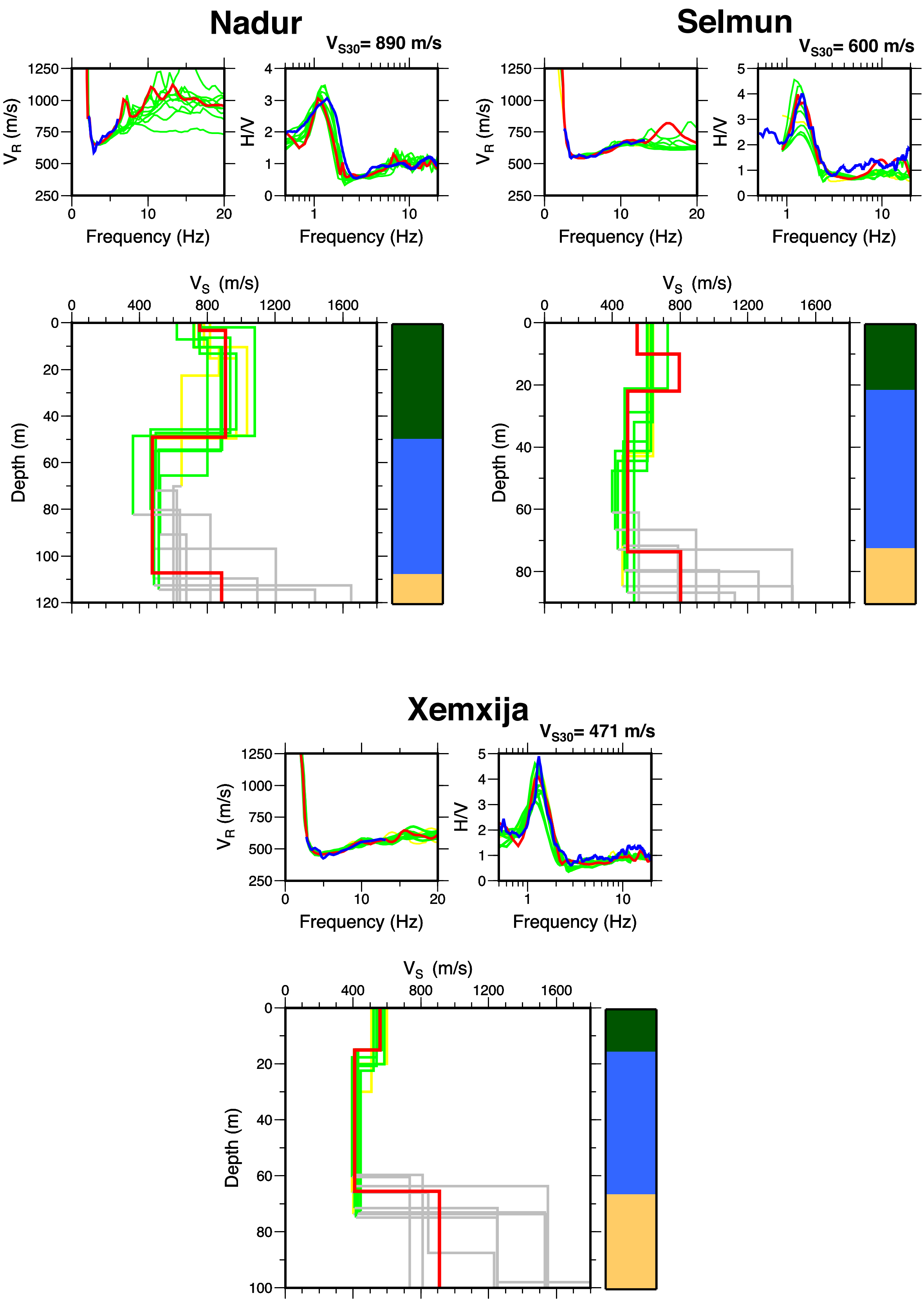

Figure 6 (*Continued.*) The joint inversion results and stratigraphic interpretation for Nadur, Selmun and Xemxija sites.

Table 2. The UCL and BC shear wave velocity values obtained for the best-fitting models and the ranges (in brackets) given by all the best-fit models of the 10 inversions.

Site	Best model UCL V_S (Range) (m s^{-1})	Best model BC V_S (Range) (m s^{-1})
Bahrija	800 (610–890)	490 (410–540)
Mdina	700 (580–860)	410 (360–460)
Mellieha	800 (800–980)	550 (470–630)
Mgarr	1070 (950–1160)	520 (380–530)
Nadur	900 (760–1080)	480 (370–660)
Selmun	700 (600–720)	490 (400–530)
Xemxija	560 (500–600)	400 (390–460)

when the BC layer is found outcropping (between 300 and 400 m s^{-1}; Panzera *et al.* 2013; Vella *et al.* 2013). A variation can also be observed in the UCL shear wave velocity, which is generally around 700–900 m s^{-1} but drops to about 560 m s^{-1} in Xemxija. Such a low velocity reflects the effect of the fractured nature of the UCL at this site. In Mgarr, a shear wave velocity of 1070 m s^{-1} was obtained for the UCL which can be tentatively related to the different geological facies of this layer and can be further studied by conducting active source measurements (such as MASW).

The V_{S30} values of the best models were also calculated and are displayed in each of the figures. The resulting values classify Mellieha and Nadur as a class A (i.e. rock site), and the rest as class B sites (i.e. deposits of very dense sand, gravel, or very stiff clay) according to the EC8 classification (Bisch *et al.* 2012). However, the presence of resonance peaks in the H/V curves indicate possible amplification phenomena, due to the buried BC, which need to be accounted for in site response studies. In general, if the low-velocity layer is present at depths exceeding 30 m (such as in Mellieha and Nadur), it does not contribute to the V_{S30} calculation, and the site is classified as a hard rock site. Taking Mgarr (Fig. 6) as an example, the V_{S30} is 670 m s^{-1}, but the average velocity decreases to 570 m s^{-1} when calculated over 70 m. Thus, as also indicated by other studies, the V_{S30} cannot be considered as a good proxy for sites where a low-velocity layer is buried in the lithostratigraphy. This highlights the importance of devising and implementing site classification schemes that are more appropriate in these situations, such as those proposed by Luzi *et al.* (2011) and Di Alessandro *et al.* (2012), which are based on the predominant frequency, f_0 or a combination of the V_{S30} and f_0.

Finally, the theoretical individual Rayleigh-wave dispersion curves up to the second higher mode were computed for the best-fit models so as to compare with the observed effective dispersion curve. In Fig. 7, we present the plots for the Bahrija and Mdina models, including the computed theoretical effective dispersion curve, which fits very well with the observed data. These examples confirm that the effective Rayleigh mode is indeed the superposition of different modes: in particular, it is possible to note that the higher modes play an important role in the frequency range when this curve shows an inversely dispersive character.

5 CONCLUSIONS

Passive seismic surface wave measurements have been used to obtain 1-D, shear wave velocity profiles at seven sites on the Maltese islands which are characterized by a thick buried clay layer in the subsurface, creating a prominent velocity inversion in the stratigraphy. The H/V technique revealed a ubiquitous fundamental frequency between 1 and 2 Hz with variable amplitudes. Such values coincide with resonance frequencies of typical 5–10 storey buildings, which are becoming increasingly common in the northern part of the islands where the clay is present.

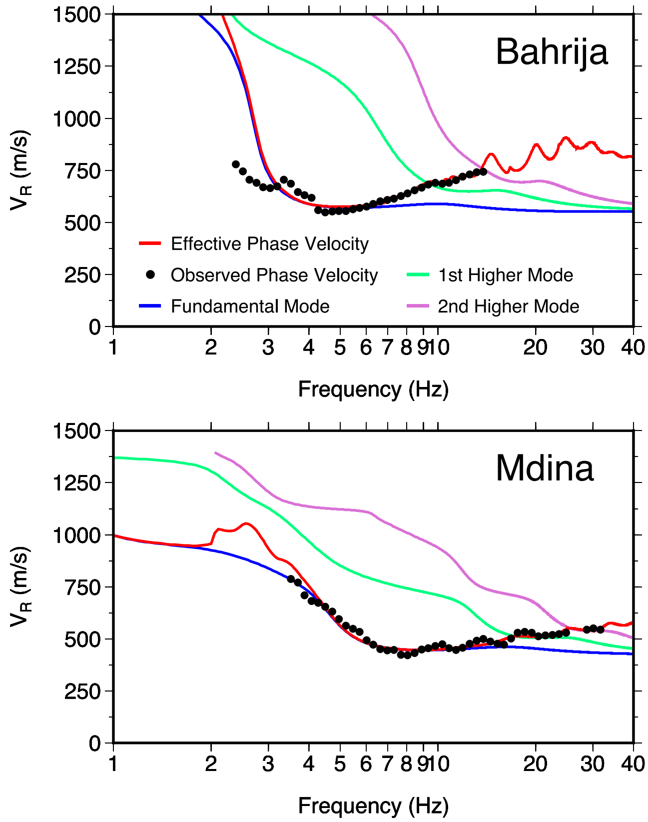

Figure 7. Comparison of the observed Rayleigh-wave phase velocities (black dots) with the theoretical effective phase velocities and the first three Rayleigh-wave modes for the Bahrija and Mdina sites.

This study justifies the use of the ESAC method, the joint inversion and genetic inversion algorithm which have been shown to perform very well in resolving both the presence and the characteristics of a low-velocity layer in the stratigraphy. The effective dispersion curves obtained using the ESAC method showed an inversely dispersive segment, related to the velocity inversion and indicating the possible presence of higher mode surface waves (Fig. 7). The analysis conducted at the only site on the islands where the BC layer is missing in the layer package provided a good example at showing that the features (both of the H/V and effective dispersion curves) obtained at the other seven sites can be attributed to the presence of the soft buried BC layer since the features were not present in the San Leonardo case. Such results continue to highlight the applicability and use of microtremor methods in obtaining good V_S profiles, not only in simple geological cases, but also in more challenging ones.

Even though the islands can be considered as having a low-to-moderate seismic hazard and the last damaging earthquake occurred more than a century ago, expansion of the building footprint onto geologically vulnerable areas and characteristic construction techniques impart a high risk to the islands, even at moderate ground shaking. This study presents an important step towards a holistic seismic risk assessment which is crucial for the islands, and adoption of an appropriate seismic building code. The shear wave velocities in the BC and UCL have been shown to vary regionally over the islands, confirming the need for more site-specific measurements. The results from this study will serve as an input to the mapping of ground motion scenarios which will shed light on possible amplification effects from potential earthquakes on areas characterized by a major velocity inversion in the stratigraphy, known to exist in many other areas. More microzonation studies, numerical modelling and investigations on the behaviour of buildings are also underway.

ACKNOWLEDGEMENTS

The authors are grateful to Dr D. Albarello and Dr E. Lunedei for the use of the ESAC and joint inversion codes, help and comments. We thank Dr Matthew R. Agius and the two reviewers, Dr Benjamin Edwards and Prof Michael Asten for insightful comments that helped us to improve the manuscript. Some figures were created using the Generic Mapping Tools (Wessel & Smith 1998). One of us (EP) was supported by Regional PhD Course in Earth Sciences 'Pegaso' (Regione Toscana, Italy). The study formed part of the SIMIT project (Integrated Italy-Malta Cross-Border System of Civil Protection) (B1-2.19/11) part-financed by the European Union under the Italia-Malta Cross-Border Cooperation Programme, 2007–2013.

REFERENCES

Agius, M.R., D'Amico, S. & Galea, P., 2015. The Easter Sunday 2011 earthquake swarm off-shore Malta: analysis on felt reports, in *Earthquakes and Their Impact on Society*, ed. D'Amico, S., Springer.

Albarello, D., Cesi, C., Eulilli, V., Guerrini, F., Lunedei, E., Paolucci, E., Pileggi, D. & Puzzilli, L.M., 2011. The contribution of the ambient vibration prospecting in seismic microzoning: an example from the area damaged by the April 6, 2009 L'Aquila (Italy) earthquake, *Boll. Geofis. Teor, Appl.,* **52,** 513–538.

Arai, H. & Tokimatsu, K., 2004. S-wave velocity profiling by inversion of microtremor H/V spectrum, *Bull. seism. Soc. Am.,* **94,** 53–63.

Arai, H. & Tokimatsu, K., 2005. S-wave velocity profiling by joint inversion of microtremor dispersion curve and Horizontal-to-Vertical (H/V) spectrum, *Bull. seism. Soc. Am.,* **95,** 1766–1778.

Asten, M.W., 2006. Site shear velocity profile interpretation from microtremor array data by direct fitting of SPAC curves, in *Proceedings of the Third International Symposium on the Effects of Surface Geology on Seismic Motion (ESG2006),* Vol. 2, pp. 1069–1082, eds Bard, P.-Y., Chaljub, E., Cornou, C., Cotton, F. & Gueguen, P., Grenoble, France, 2006 August 30–September 1, LCPC.

Asten, M.W., Askan, A., Ekincioglu, E.E., Sisman, F.N. & Ugurhan, B., 2014. Site characterisation in north-western Turkey based on SPAC and HVSR analysis of microtremor noise, *Explor. Geophys.,* **45,** 74–85.

Bard, P.Y. & SESAME-Team, 2005. Guidelines for the implementation of the H/V spectral ratio technique on ambient vibrations: measurements, processing, and interpretations, in *SESAME European Research Project,* WP12, deliverable D23.12, 2004. Available at: http://sesame-fp5.obs.ujf-grenoble.fr/Deliverables2004.

Bisch, P. *et al.*, 2012. *Eurocode8: Seismic Design of Buildings,* Worked examples, Publications Office of the European Union.

Bonnefoy-Claudet, S., Cornou, C., Bard, P.-Y., Cotton, F., Moczo, P., Kristek, J. & Fäh, D., 2006. H/V ratio: a tool for site effects evaluation. Results from 1-D noise simulations, *Geophys. J. Int.,* **167,** 827–837.

Boore, D., 2015. Notes on relating density to velocity for use in site amplification calculations. Available at: http://www.daveboore.com/daves_notes/daves_notes_on_relating_density_to_velocity_v3.0.pdf, last accessed 24 August 2015.

Capon, J., 1969. High-resolution frequency–wavenumber spectrum analysis, *Proc. IEEE,* **57,** 1408–1418.

Castellaro, S. & Mulargia, F., 2009. The effect of velocity inversions on H/V, *Pure appl. Geophys.,* **166,** 567–592.

Castellaro, S., Mulargia, F. & Rossi, P.M., 2008. VS30: proxy for seismic amplification?, *Seismol. Res. Lett.,* **79,** 540–542.

Di Alessandro, C., Bonilla, L.B., Boore, D.M., Rovelli, A. & Scotti, O., 2012. Predominant-period site classification for response spectra prediction equations in Italy, *Bull. seism. Soc. Am.,* **102,** 680–695.

Di Giacomo, D., Gallipoli, M.R., Mucciarelli, M., Parolai, S. & Richwalski, S.M., 2005. Analysis and modeling of HVSR in the presence of a velocity inversion: the case of Venosa, Italy, *Bull. seism. Soc. Am.,* **95,** 2364–2372.

Fäh, D., Kind, F. & Giardini, D., 2003. Inversion of local S-wave velocity structures from average H/V ratios, and their use for the estimation of site-effects, *J. Seismol.,* **7,** 449–467.

Foti, S., Lai, C.G., Rix, G.J. & Strobbia, C., 2015. *Surface Wave Methods for Near-Surface Site Characterization*, CRC Press.

Galea, P., 2007. Seismic history of the Maltese islands and considerations on seismic risk, *Ann. Geophys.,* **50,** 725–740.

Galea, P., D'Amico, S. & Farrugia, D., 2014. Dynamic characteristics of an active coastal spreading area using ambient noise measurements—Anchor Bay, Malta, *Geophys. J. Int.,* **199,** 1166–1175.

Gallipoli, M.R. & Mucciarelli, M., 2009. Comparison of site classification from VS30, VS10, and HVSR in Italy, *Bull. seism. Soc. Am.,* **99,** 340–351.

Gigli, G., Frodella, W., Mugnai, F., Tapete, D., Cigna, F., Fanti, R., Intrieri, E. & Lombardi, L., 2012. Instability mechanisms affecting cultural heritage sites in the Maltese Archipelago, *Nat. Hazards Earth Syst. Sci.,* **12,** 1883–1903.

Government of Malta, 1958. *Reports on Geological Investigation of the Maltese Islands,* R. Costain Ltd.

Hayashi, K., Cakir, R. & Walsh, T.J., 2016. Comparison of dispersion curves obtained by active and passive surface wave methods: examples from seismic site characterization surveys for school seismic safety evaluations in Thurston County, Washington, in *SAGEEP 2016*, Denver, Colorado, USA.

Ikeda, T., Matsuoka, T., Tsuji, T. & Hayashi, K., 2012. Multimode inversion with amplitude response of surface waves in the spatial autocorrelation method, *Geophys. J. Int.,* **190,** 541–552.

Lunedei, E. & Albarello, D., 2009. On the seismic noise wavefield in a weakly dissipative layered Earth, *Geophys. J. Int.,* **177,** 1001–1014.

Luzi, L., Puglia, R., Pacor, F., Gallipoli, M.R., Bindi, D. & Mucciarelli, M., 2011. Proposal for a soil classification based on parameters alternative or complementary to Vs,30, *Bull. Earthq. Eng.,* **9,** 1877–1898.

Nakamura, Y., 1989. A method for dynamic characteristics estimations of subsurface using microtremors on the ground surface, *Q. Rep. Railw. Tech. Res. Inst. Nguyen,* **30,** 25–33.

Nakamura, Y., 2000. Clear identification of fundamental idea of Nakamura's technique and its applications, in *12th World Conference on Earthquake Engineering 2000,* Auckland, New Zealand.

Ohori, M., Nobata, A. & Wakamatsu, K., 2002. A comparison of ESAC and FK methods of estimating phase velocity using arbitrarily shaped microtremor arrays, *Bull. seism. Soc. Am.,* **92,** 2323–2332.

Okada, H., 2003. *The Microtremor Survey Method,* Geophysical Monograph Series No. 12, Society of Exploration Geophysicists.

Pace, S., Panzera, F., D'Amico, S., Galea, P. & Lombardo, G., 2011. Modelling of ambient noise HVSR in a complex geological area- Case study of the Xemxija Bay Area, Malta, in *Riassunti Estesi Delle Comunicazioni, 30° Convegno Nazionale GNGTS*, pp. 299–302, eds Slejko, D. & Rebez, A., Trieste, Italy.

Panzera, F. & Lombardo, G., 2012. Seismic property characterization of lithotypes cropping out in the Siracusa urban area, Italy, *Eng. Geol.,* **153,** 12–24.

Panzera, F., D'Amico, S., Lotteri, A., Galea, P. & Lombardo, G., 2012. Seismic site response of unstable steep slope using noise measurements: the case study of Xemxija Bay area, Malta, *Nat. Hazards Earth Syst. Sci.,* **12,** 3421–3431.

Panzera, F., D'Amico, S., Galea, P., Lombardo, G., Gallipoli, M.R. & Pace, S., 2013. Geophysical measurements for site response investigation: preliminary results on the island of Malta, *Boll. Geofis. Teor. Appl.,* **54,** 111–128.

Parolai, S., Picozzi, M., Richwalski, S.M. & Milkereit, C., 2005. Joint inversion of phase velocity dispersion and H/V ratio curves from seismic noise recordings using a genetic algorithm, considering higher modes, *Geophys. Res. Lett.,* **32,** doi:10.1029/2004GL021115.

Parolai, S., Richwalski, S.M., Milkereit, C. & Fäh, D., 2006. S-wave velocity profiles for earthquake engineering purposes for the Cologne area (Germany), *Bull. Earthq. Eng.,* **4,** 65–94.

Pedley, M., 2011. The Calabrian Stage, Pleistocene highstand in Malta: a new marker for unravelling the Late Neogene and Quaternary history of the islands, *J. geol. Soc. Lond.,* **168**(4), 913–926.

Pedley, M., Clarke, M. & Galea, P., 2002. *Limestone Isles in a Crystal Sea: The Geology of the Maltese Islands,* Publishers Enterprises Group Ltd.

Picozzi, M. & Albarello, D., 2007. Combining genetic and linearized algorithms for a two-step joint inversion of Rayleigh wave dispersion and H/V spectral ratio curves, *Geophys. J. Int.,* **169,** 189–200.

Picozzi, M., Parolai, S. & Albarello, D., 2005. Statistical analysis of noise Horizontal to Vertical Spectral Ratios (HVSR), *Bull. seism. Soc. Am.,* **95,** 1779–1786.

Picozzi, M., Strollo, A., Parolai, S., Durukal, E., Özel, O., Karabulut, S., Zschau, J. & Erdik, M., 2009. Site characterization by seismic noise in Istanbul, Turkey, *Soil Dyn. Earthq. Eng.,* **29,** 469–482.

Satoh, T., Kawase, H. & Matsushima, S., 2001. Differences between site characteristics obtained from microtremors, S-waves, P-waves and codas, *Bull. seism. Soc. Am.,* **91,** 313–334.

Scherbaum, F., Hinzen, K.-G. & Ohrnberger, M., 2003. Determination of shallow shear wave velocity profiles in the Cologne, Germany area using ambient vibrations, *Geophys. J. Int.,* **152,** 597–612.

Shabani, E., Cornou, C., Haghshenas, E., Wathelet, M., Bard, P.-Y., Mirzaei, N. & Eskandari-Ghadi, M., 2008. Estimating shear-waves velocity structure by using array methods (FK and SPAC) and inversion of ellipticity curves at a site in south of Tehran, in *The 14th World Conference on Earthquake Engineering,* Beijing, China.

Tokimatsu, K., 1997. Geotechnical site characterization using surface wave, in *Earthquake Geotechnical Engineering*, pp. 1333–1368, ed. Ishihara, K., Balkema.

Vella, A., Galea, P. & D'Amico, S., 2013. Site frequency response characterisation of the Maltese islands based on ambient noise H/V ratios, *Eng. Geol.,* **163,** 89–100.

Wessel, P. & Smith, W.H., 1998. New, improved version of generic mapping tools released, *EOS, Trans. Am. geophys. Un.,* **79,** 579, doi:10.1029/98EO00426.

Xia, J., Miller, R.D. & Park, C.B., 1999. Estimation of near-surface shear-wave velocity by inversion of Rayleigh wave, *Geophysics,* **64,** 691–700.

Xia, J., Miller, R.D., Park, C.B. & Tian, G., 2003. Inversion of high frequency surface waves with fundamental and higher modes, *J. Appl. Geophys.,* **52,** 45–57.

Yamanaka, H. & Ishida, H., 1996. Application of genetic algorithms to an inversion of surface-wave dispersion data, *Bull. seism. Soc. Am.,* **86,** 436–444.

Zammit-Maempel, G., 1977. *An Outline of Maltese Geology,* Progress Press.

Zhang, B. & Lu, L., 2003. Rayleigh wave and detection of low-velocity layers in a stratified half-space, *Acoust. Phys.,* **49,** 516–528.

Zor, E., Özalaybey, S., Karaaslan, A., Tapirdamaz, M.C., Özalaybey, S.C., Tarancioğlu, A. & Erkan, B., 2010. Shear wave velocity structure of the Izmit Bay area (Turkey) estimated from active-passive array surface wave and single-station microtremor methods, *Geophys. J. Int.,* **182,** 1603–1618.